

Tasquinimod enhances the sensitivity of ovarian cancer cells to cisplatin by regulating the Nur77-Bcl-2 apoptotic pathway

Ying Lin^{1,A,B,D–F}, Ya-Qiong Liu^{2,A–D,F}, Ke-An Zhu^{1,B,C,E,F}, Meng-Qi Hu^{1,B–D,F}, Zhao Li^{1,B–D,F}, Xiao-Jia Min^{1,A,B,E,F}

¹ Department of Gynecology, The First Affiliated Hospital of Hunan Normal University, Changsha, China

² Department of Gynecology and Obstetrics, Guangzhou Women and Children's Medical Center, Guangzhou Medical University, China

A – research concept and design; B – collection and/or assembly of data; C – data analysis and interpretation;

D – writing the article; E – critical revision of the article; F – final approval of the article

Advances in Clinical and Experimental Medicine, ISSN 1899–5276 (print), ISSN 2451–2680 (online)

Adv Clin Exp Med. 2024;33(2):151–161

Address for correspondence

Xiao-Jia Min

E-mail: Minminjia2022@163.com

Funding sources

This work was supported by the Clinical Medical Technology Innovation Guide Project of Hunan Province (grant No. 2020SK50905).

Conflict of interest

None declared

Received on September 30, 2022

Reviewed on December 5, 2022

Accepted on May 9, 2023

Published online on July 28, 2023

Cite as

Lin Y, Liu YQ, Zhu KA, Hu MQ, Li Z, Min XJ. Tasquinimod enhances the sensitivity of ovarian cancer cells to cisplatin by regulating the Nur77-Bcl-2 apoptotic pathway.

Adv Clin Exp Med. 2024;33(2):151–161.

doi:10.17219/acem/166044

DOI

10.17219/acem/166044

Copyright

Copyright by Author(s)

This is an article distributed under the terms of the Creative Commons Attribution 3.0 Unported (CC BY 3.0) (<https://creativecommons.org/licenses/by/3.0/>)

Abstract

Background. Resistance to cisplatin (DDP) in ovarian cancer therapy has been a major clinical barrier. Drug-resistant cancers have been shown to downregulate the proapoptotic protein B-cell lymphoma-2 (Bcl-2) to inhibit apoptosis. Therefore, we explored whether tasquinimod could modulate resistance to DDP through apoptotic pathways.

Objectives. We aimed to explore the relationship between tasquinimod, Nur77-Bcl-2 apoptosis pathway and sensitivity of the ovarian carcinoma cell line SKOV3 and the DDP-resistant strain SKOV3/DDP cells to DDP.

Materials and methods. First, SKOV3 and SKOV3/DDP cells were treated with 2 µg/mL DDP or 40 µM tasquinimod. Western blot and quantitative real-time polymerase chain reaction (qPCR) were then used to analyze the expression of histone deacetylase 4 (HDAC4), Nur77, Bcl-2 (BH3 domain-specific), and caspase-3. Flow cytometry, scratch-wound assay and immunofluorescence were used to detect apoptosis, migration rate, and related expression of Nur77 and Bcl-2 (BH3 domain-specific). Subsequently, 5×10⁷ SKOV3 or SKOV3/DDP cells cultured with 2 µg/mL DDP were injected into 4-week-old female BALB/c nude mice. Then, the mice were administered 4 mg/kg DDP and 50 mg/kg tasquinimod every 3 days. Finally, the changes in tumor diameter and weight were measured.

Results. After treatment of SKOV3 and SKOV3/DDP cells with tasquinimod, cell migration and HDAC4 expression levels were significantly reduced, while Nur77 expression was increased. Tasquinimod treatment enhanced the expression of Nur77 and caspase-3, and cells transfected with si-Nur77 showed the opposite result. Transfection of si-Nur77 reduced the expression of caspase-3 and Nur77 in the SKOV3/DDP cells that were treated with both DDP and tasquinimod. After injection of SKOV3/DDP cells into the mice, the tumor diameter, mass and in vivo HDAC4 level were significantly decreased by tasquinimod. Meanwhile, the levels of Nur77 and Bcl-2 (BH3 domain-specific) were increased.

Conclusions. Tasquinimod upregulated the Nur77/Bcl-2 pathway to induce apoptosis in SKOV3/DDP cells and enhanced the anti-tumor effect of DDP in SKOV3/DDP xenografts. Therefore, tasquinimod can be expected to find clinical applications in enhancing DDP resistance.

Key words: ovarian cancer, resistance to cisplatin (DDP), tasquinimod, Nur77-Bcl-2 pathway

Background

Ovarian cancer is considered one of the deadliest gynecological malignancies worldwide,¹ with most patients presenting at an advanced stage due to a lack of formal screening and early detection methods.² Currently, the standard treatment for ovarian cancer is chemotherapy and cytoreductive surgery,^{3,4} with the initial adjuvant treatment being platinum-based drugs such as cisplatin (DDP) or carboplatin.¹ Cisplatin interferes with DNA repair mechanisms by cross-linking DNA purine bases, thus inducing apoptosis in cancer cell.⁵ Although DDP has been for decades a key chemotherapeutic drug for treating patients with different forms of tumors, drug resistance is a major clinical barrier.⁶

Cancer cells often evade apoptosis by upregulating the anti-apoptotic protein B-cell lymphoma 2 (Bcl-2), while drug-resistant cancers downregulate or inactivate pro-apoptotic proteins to inhibit apoptosis.⁷ The level of Bcl-2 increases in DDP-resistant ovarian cancer cell lines compared with non-resistant cells,⁸ and the overexpression of Bcl-2 increases the cell growth and apoptosis inhibition of DDP-induced SKOV3 cells.⁹

It is widely known that Bcl-2 exposes its Bcl-2 (BH3 domain-specific) after binding to orphan nuclear receptor 4A1 (Nur77),¹⁰ resulting in the conversion of the original anti-apoptotic effect to a proapoptotic effect.¹¹ This interaction with Nur77 is mediated by the N-terminal ring region of Bcl-2, and this action is required for the apoptosis of cancer cells that is induced by many anti-tumor drugs.¹⁰ In ovarian cancer tissue microarrays, the expression of Nur77 was significantly reduced in platinum-resistant tumors.¹² While Nur77 binds Bcl-2 to induce its conformational change and exposes its BH3 domain, resulting in the proapoptotic effect of Bcl-2,¹⁰ this effect has not been investigated in DDP-resistant ovarian cancer.

Interestingly, histone deacetylase 4 (HDAC4) binds to the transcriptional regulatory region of the *Nur77* gene.¹³ Deacetylation of histones occurs through HDAC, which is abnormal in many types of cancer,^{14,15} and histone acetylation significantly affects the transcription of target genes.¹³ Moreover, HDAC4 can regulate tumorigenesis by remodeling the chromatin structure and controlling protein entry onto DNA.¹⁴ Additionally, HDAC inhibitors enhance radiation-induced cell death and reduce DNA double-strand breaks, leading to increased apoptosis,¹⁴ which suggests that HDAC may play a role in the disease process.^{14,15}

Tasquinimod is an analog of the HDAC inhibitor BML-210.¹⁶ It prevents HDAC4-dependent recruitment of MEF2 to DNA, thereby increasing the expression of the target gene *Nur77*.^{17,18} Tasquinimod, a quinoline 3-carboxamide derivative, has shown structural similarity to kynurenic acid (KYNA), an endogenous tryptophan metabolite,^{15,20} and is primarily considered an anti-cancer drug.¹⁹ Therefore, it is reasonable to speculate that the lack of Nur77 can convert the anti-apoptotic function of Bcl-2 to proapoptotic.

Objectives

There is currently no research regarding the effect of tasquinimod on the DDP sensitivity of ovarian cancer cell lines. Therefore, this study aims to explore the relationship between tasquinimod, the Nur77-Bcl-2 apoptosis pathway and the DDP sensitivity of ovarian cancer cell lines.

Materials and methods

Cell culture and treatment

First, the normal human ovarian epithelial cell IOSE80 was obtained from Shanghai Huiying Biotech (Shanghai, China), and the ovarian carcinoma cell line SKOV3 and the DDP-resistant strain SKOV3/DDP cells were produced by American Type Culture Collection (ATCC; Manassas, USA). The IOSE80,²¹ SKOV3²² and SKOV3/DDP²³ cells were cultured in Roswell Park Memorial Institute (RPMI)-1640 medium containing 10% fetal bovine serum (FBS) at 37°C with 5% CO₂.⁴ The cells were passaged at a ratio of 1:3 to 1:4, and they were in the log phase for subsequent experiments.

The cells were divided into 11 groups and then treated as follows: 1) SKOV3 group – SKOV3 cells without treatment; 2) SKOV3+tasquinimod group – SKOV3 cells treated with 40 µM tasquinimod²⁴; 3) SKOV3/DDP group – SKOV3/DDP cells without any treatment; 4) SKOV3/DDP+tasquinimod group – SKOV3/DDP cells treated with 40 µM tasquinimod; 5) SKOV3+DDP group – SKOV3 cells treated with 2 µg/mL DDP²³; 6) SKOV3/DDP+DDP group – SKOV3/DDP cells treated with 2 µg/mL DDP; 7) SKOV3/DDP+DDP+tasquinimod group – SKOV3/DDP cells treated with 2 µg/mL DDP and 40 µM tasquinimod.

The last 4 groups were treated with tasquinimod or DDP after being transfected with expression vectors according to the manufacturer's protocol. The negative siRNA (si-NC) or Nur77 siRNA (si-Nur77) (Shanghai GenePharma Co., Ltd., Shanghai, China) was transfected into SKOV3/DDP cells using Lipofectamine® 2000 (Invitrogen, Thermo Fisher Scientific, Waltham, USA).^{8,25} The transfected cell groups were as follows: 8) SKOV3/DDP+DDP+si-NC group – SKOV3/DDP cells cultured with 2 µg/mL DDP after being transfected with si-NC; 9) SKOV3/DDP+DDP+tasquinimod+si-NC group – SKOV3/DDP cells cultured with 40 µM tasquinimod and 2 µg/mL DDP after being transfected by si-NC; 10) SKOV3/DDP+DDP+si-Nur77 group – SKOV3/DDP cells cultured with 2 µg/mL DDP after transfection with si-Nur77; and 11) SKOV3/DDP+DDP+tasquinimod+si-Nur77 group – SKOV3/DDP cells cultured with 2 µg/mL DDP and 40 µM tasquinimod after being transfected with si-Nur77. All groups cultured with 40 µM tasquinimod or 2 µg/mL DDP were treated for 24 h.

Animals

The SKOV3 or SKOV3/DDP cells (5×10^7) were subcutaneously injected into 4-week-old female BALB/c nude mice.^{26,27} To explore the role of tasquinimod, we divided the nude mice into 3 groups, namely SKOV3+DDP, SKOV3/DDP+DDP and SKOV3/DDP+DDP+tasquinimod. The SKOV3+DDP group was subcutaneously injected with 5×10^7 SKOV3 cells after being treated with 2 $\mu\text{g/mL}$ DDP for 48 h, and then 4 mg/kg DDP was injected every 3 days. The SKOV3/DDP+DDP group was subcutaneously injected with 5×10^7 SKOV3/DDP cells after being cultured with 2 $\mu\text{g/mL}$ DDP for 48 h, and then 4 mg/kg DDP was injected every 3 days. The SKOV3/DDP+DDP+tasquinimod group was subcutaneously injected with 5×10^7 SKOV3/DDP cells after being cultured with 2 $\mu\text{g/mL}$ DDP for 48 h, then 4 mg/kg DDP and 50 mg/kg tasquinimod were injected every 3 days. All mice were sacrificed, and tumor lesions were excised after 5 weeks. Next, images of mice and tumors were obtained from Shanghai Laboratory Animal Research Center (Shanghai, China), which was approved by China Medical University Animal Care and Use Committee, and complied with national criteria on experimental procedures on animals.

Cell Counting Kit-8 (CCK-8)

The cells (logarithmic phase) were seeded at a density of 2.5×10^3 into a well for 24 h. The CCK-8 reagent (NU679; Dojindo Laboratories, Rockville, USA) was added to the wells and then incubated for 1 h at 37°C.²⁸ The absorbance of the sample at 450 nm was detected using a microplate reader, and each group was tested 3 times.

Scratch-wound assay²⁹

Cells were seeded at a density of 1×10^5 cells/well on 1% gelatin-coated six-well plates (Corning, Cambridge, USA). The linear wounds were scratched using a sterile pipette tip. The monolayers were then washed with phosphate-buffered saline (PBS) to clear away floating cells. After 24 h or 48 h of incubation with RPMI-1640 media, cell migration was assessed using inverted biological microscope (model DSZ2000X; Cnmicro, Beijing, China). All experiments were performed independently in triplicate. Each group was tested 3 times.

Detection of cell apoptosis by flow cytometry

Collected cells were washed once with PBS and treated with Annexin V-FITC Apoptosis Detection Kit (KGA108; Nanjing KeyGen Biotech, Nanjing, China).³⁰ Briefly, the binding buffer was used to suspend cells; then, Annexin V-FITC and propidium iodide were added for 10 min

in the dark. A flow cytometer (A00-1-1102; Beckman Coulter, Brea, USA) was used to analyze apoptosis.³¹ Each group was tested 3 times.

Immunofluorescence

The distribution and level of Nur77³² and Bcl-2 (BH3 domain-specific)³³ were detected with immunofluorescence (IF) staining. Cells were fixed in 4% paraformaldehyde for 15 min, washed with PBS and permeabilized with 0.1% Triton X-100. Next, bovine serum albumin (BSA) was used to block the non-specific antigens at room temperature, and an anti-Nur77 antibody (#3960s; Cell Signaling Technology, Danvers, USA) or an anti-Bcl-2 antibody (ab32445; Abcam, Waltham, USA) was applied overnight at 4°C. After washing with PBS, secondary anti-rabbit IgG (H+L) antibodies were applied. Finally, the nucleus was visualized with 4',6-diamidino-2-phenylindole (DAPI), and cells were observed under a fluorescence microscope (model BA210T; Motic, Xiamen, China). Each group was tested 3 times.

Quantitative real-time polymerase chain reaction (qPCR)

Total RNA (cells or tissues) was separated using the TRIzol method. RevertAid™ First Strand cDNA Synthesis Kit (CW2569; Beijing Comwin Biotech, Beijing, China) was used to transcribe cDNA.³⁴ Primer sequences of β -actin, HDAC4 and Nur77 were purchased from Sangon Biotech (Shanghai, China) (Table 1).³⁵ Next, a fluorescent quantitative PCR instrument (PikoReal™; Thermo Fisher Scientific) was used to measure gene expression.³⁶ The $2^{-\Delta\Delta CT}$ method was applied to assess the relative mRNA level³⁷ concerning β -actin. Each group was tested 4 times.

Table 1. The primer sequence

| Primer ID | 5'-3' |
|------------------|------------------------|
| β -actin-F | ACCTGAAGTACCCCATCGAG |
| β -actin-R | AGCACAGCTGGATAGCAAC |
| HDAC4-F | CTTGTTGGTTACCTGGCTCA |
| HDAC4-R | TCCAACGAGCTCCAAACTCC |
| Nur77-F | CCTGGTGAAGCTTTGGTATGGA |
| Nur77-R | GCCTTGCCAACACATTAT |

Western blot

Total protein was obtained by centrifuging each sample at 10,000 g for 10 min at 4°C. Then, a bicinchoninic acid (BCA) protein kit was used to measure the protein level.³⁸ Sodium dodecyl sulfate-polyacrylamide gel electrophoresis (SDS-PAGE) (12%) was used to separate total proteins with 100 mV power. Proteins were then transferred to a polyvinylidene difluoride (PVDF) membrane at 300 mA power.

Then, a 5% nonfat skim milk powder-Tween 0.1% solution was applied to block membranes. Antibodies against HDAC4 (668381-Ig, 1:3000; Proteintech, San Diego, USA), Nur77 (12235-1-AP, 1:1000; Proteintech), caspase-3 (#9661, 1:1000; Cell Signaling Technology, Danvers, USA), Bcl-2 (BH3 domain-specific) (AP1303a, 1:1000; Abcepta Biotech Ltd. Co., Suzhou, China), PCNA (10205-2-AP, 1:5000; Proteintech), and β -actin (66009-1-Ig, 1:5000; Proteintech) were added. Samples were washed, and the secondary antibody HRP goat anti-mouse IgG (SA00001-1, 1:5000; Proteintech) or HRP goat anti-rabbit IgG (SA00001-2, 1:6000; Proteintech) was applied to the membrane. The protein samples were assessed using chemiluminescence imaging system.³⁹ The internal reference was PCNA or β -actin.⁴⁰ Each group was tested 4 times.

Statistical analyses

GraphPad Prism 9 (GraphPad Software, San Diego, USA) was used for statistical analysis.⁴¹ The data were presented as the mean \pm standard deviation ($M \pm SD$), and the data normality distribution was assessed with the Shapiro–Wilk test.⁴² The homogeneity of variance was tested with the F test of Student's *t*-test between the 2 groups.⁴² The Brown–Forsythe test was utilized to evaluate the homogeneity of variance between multiple groups.⁴³ Following data normality and homogeneity testing, the differences between the 2 groups were analyzed using unpaired Student's *t*-test.⁴² When the hypothesis of normality was satisfied, but the homogeneity of variance was unsatisfied, the differences between the 2 groups were analyzed using the Mann–Whitney U-test.^{44,45} When the hypothesis of normality was satisfied, the difference between multiple groups was analyzed with one-way analysis of variance (ANOVA).⁴⁶ The Tukey–Kramer post hoc test comparisons were completed if the main effects of ANOVA were statistically significant.⁴⁷

In the Shapiro–Wilk test, $p > 0.1$ demonstrated that the data conform to a normal distribution. In the F-test of Student's *t*-test and Brown–Forsythe test, $p > 0.05$

illustrated that the variance was uniform. In the Mann–Whitney U test, unpaired Student's *t*-test or one-way ANOVA test, $p < 0.05$ illustrated significant differences between the groups. No outlying data were excluded, and data were analyzed blindly. The statistical methods, results and sample size related to the figures are shown in Supplementary Tables 1–7.

Results

Expression of HDAC4 in ovarian cancer cells

To determine whether there is a difference in HDAC4 expression in different ovarian cancer cells, we examined IOSE80, SKOV3 and SKOV3/DDP cell lines. We found that HDAC4 expression in SKOV3 cells was higher than that in IOSE80 cells, and the HDAC4 level was higher in the SKOV3/DDP cells than in SKOV3 cells (Fig. 1A,B). These results illustrated that ovarian cancer resistance to DDP may be regulated by HDAC4.

Effect of tasquinimod on growth inhibition of SKOV3 or SKOV3/DDP cells

To further analyze the HDAC4 function in DDP resistance in ovarian cancer, we treated SKOV3 and SKOV3/DDP cells with 40 μ M tasquinimod (HDAC4 inhibitor). Cell viability was significantly decreased after the cells were treated with tasquinimod for 24 h or 48 h (Fig. 2A,B). Furthermore, cell mobility was negatively correlated with the addition of tasquinimod. The relative scratch width in the SKOV3+tasquinimod and SKOV3/DDP+tasquinimod groups decreased when compared to both the SKOV3 and SKOV3/DDP groups after 48 h, respectively (Fig. 3). Furthermore, we found that the HDAC4 level in SKOV3/DDP cells significantly decreased under the influence of tasquinimod, while the Nur77 level significantly increased 48 h later (Fig. 2C). These results showed that tasquinimod affected the growth inhibition rate of SKOV3 or SKOV3/DDP cells.

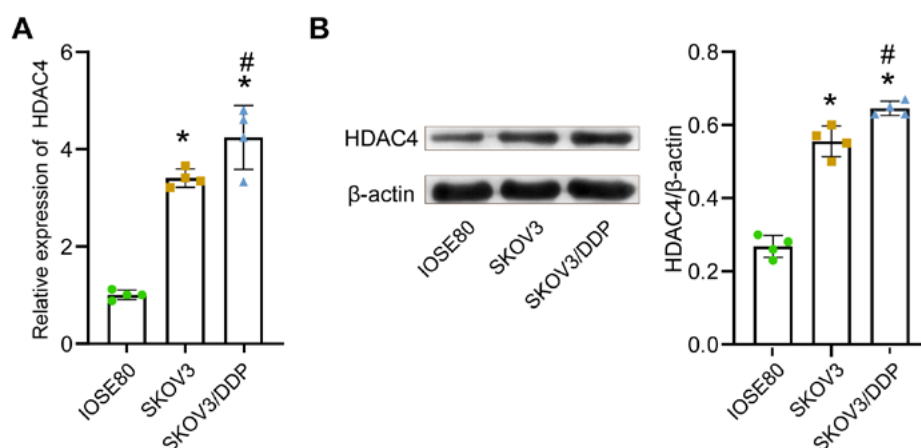


Fig. 1. Expression of histone deacetylase 4 (HDAC4) in IOSE80, SKOV3 and SKOV3/DDP cells. HDAC4 level was measured with quantitative real-time polymerase chain reaction (qPCR) (A) and western blot (B) ($n = 4$ for qPCR and western blot (both biological replicates)). Comparisons were made using the one-way analysis of variance (ANOVA) test. In the one-way ANOVA test, $p < 0.05$ illustrated significant differences between the data (* $p < 0.05$ compared to IOSE80; # $p < 0.05$ compared to SKOV3). Data are presented as mean \pm standard deviation ($M \pm SD$). The scatter point represents the value of a single sample. The details of statistical methods, results and sample size are listed in Supplementary Table 1

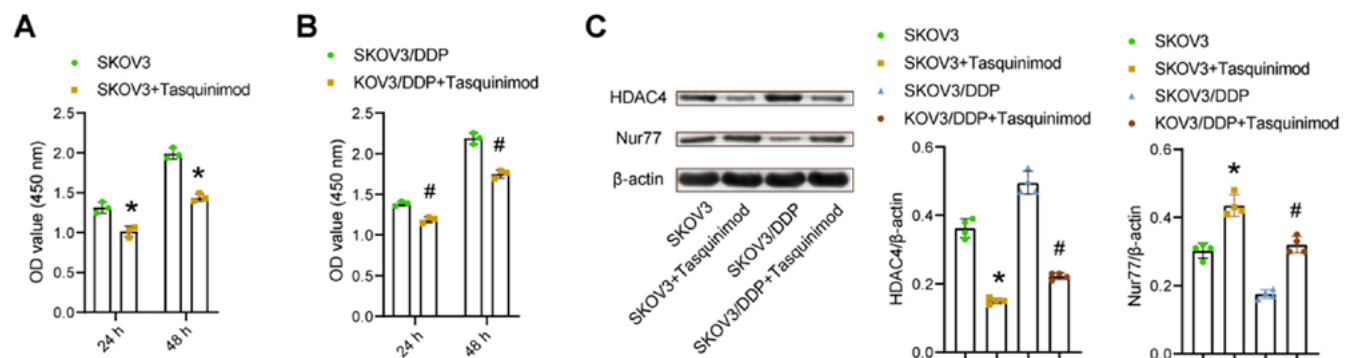


Fig. 2. Tasquinimod effect on growth inhibition rate of SKOV3 or SKOV3/DDP cells. Cell Counting Kit-8 (CCK-8) was applied to assess SKOV3 cells (A) and SKOV3/DDP cell viability (B) ($n = 3$ for CCK-8). Comparisons were made using the Student's t-test. The histone deacetylase 4 (HDAC4) and Nur77 expression was measured with western blot after cells were treated with 0.01 mmol/L tasquinimod (C) ($n = 4$ for quantitative real-time polymerase chain reaction (qPCR) and western blot (both biological replicates)). Comparisons were made using the one-way analysis of variance (ANOVA) test. In the unpaired t-test of Student's t-test or one-way ANOVA test, $p < 0.05$ illustrated significant differences between the data (* $p < 0.05$ compared to SKOV3; # $p < 0.05$ compared to SKOV3/DDP). Data are presented as mean \pm standard deviation ($M \pm SD$). The scatter point represents the value of a single sample. The details of statistical methods, results and sample size are listed in Supplementary Table 2

OD – optical density.

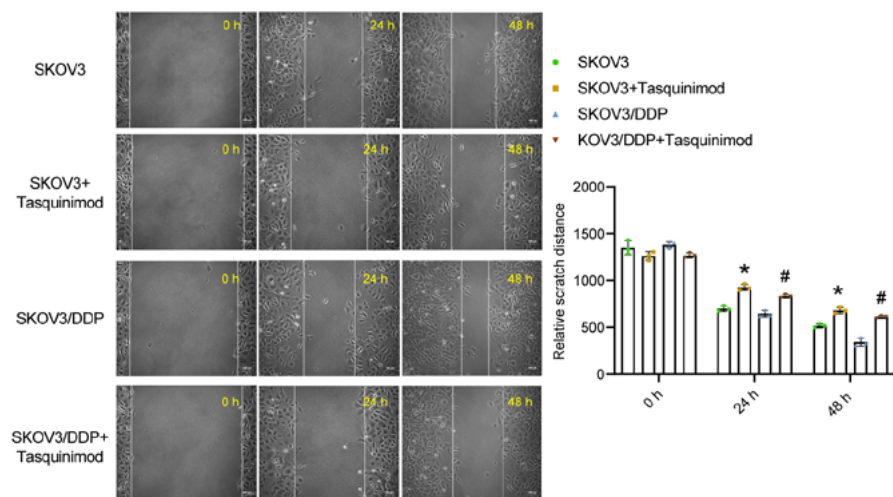


Fig. 3. Tasquinimod effect on growth inhibition rate of SKOV3 or SKOV3/DDP cells. The scratch-wound assay was utilized to measure the scratch width (* $p < 0.05$ compared to SKOV3; # $p < 0.05$ compared to SKOV3/DDP; $n = 3$ for scratch-wound assay (both biological replicates)). Comparisons were made using the one-way analysis of variance (ANOVA) test, with $p < 0.05$ illustrating significant differences between the groups (* $p < 0.05$ compared to SKOV3; # $p < 0.05$ compared to SKOV3/DDP). Data are presented as mean \pm standard deviation ($M \pm SD$). The scatter point represents the value of a single sample

Tasquinimod increased the sensitivity of SKOV3/DDP cells to DDP

Taking into consideration the influence of tasquinimod on the growth inhibition rate of SKOV3 or SKOV3/DDP, we treated cells with DDP to investigate whether tasquinimod could improve cell sensitivity to DDP. Cell viability in the SKOV3/DDP+DDP+tasquinimod group was significantly decreased compared to the SKOV3/DDP+DDP group (Fig. 4A). Furthermore, the relative scratch distance of the SKOV3/DDP+DDP+tasquinimod group was lower than that of the SKOV3/DDP+DDP group (Fig. 4B). Moreover, the apoptosis rate in the SKOV3/DDP+DDP+tasquinimod group was significantly increased when compared to the SKOV3/DDP+DDP group (Fig. 4C). After 48 h, the western blot demonstrated that the expression of capase-3 in the SKOV3/DDP+DDP+tasquinimod group significantly increased compared with the SKOV3/DDP+DDP group (Fig. 4D). These data demonstrate that

tasquinimod increased cell sensitivity to DDP while inhibiting growth and promoting apoptosis.

Tasquinimod affected the Nur77 apoptosis pathway of DDP-treated SKOV3/DDP cells

To further verify the effect of tasquinimod on the Nur77-Bcl-2 apoptotic pathway in DDP-treated SKOV3/DDP cells, we detected related mRNA and protein expression. We observed increased Nur77 and Bcl-2 (BH3 domain-specific) and decreased total Bcl-2 in SKOV3/DDP cells after the administration of tasquinimod (Fig. 5A,B). The treatment with tasquinimod induced abundant Nur77 expression in the cytoplasm (Fig. 5C). Immunofluorescence and western blot detected increased Nur77 and Bcl-2 (BH3 domain-specific), which were mainly localized in the cytoplasm (Fig. 5D,E). These results confirmed that tasquinimod affected the Nur77-Bcl-2 apoptotic pathway of SKOV3/DDP cells.

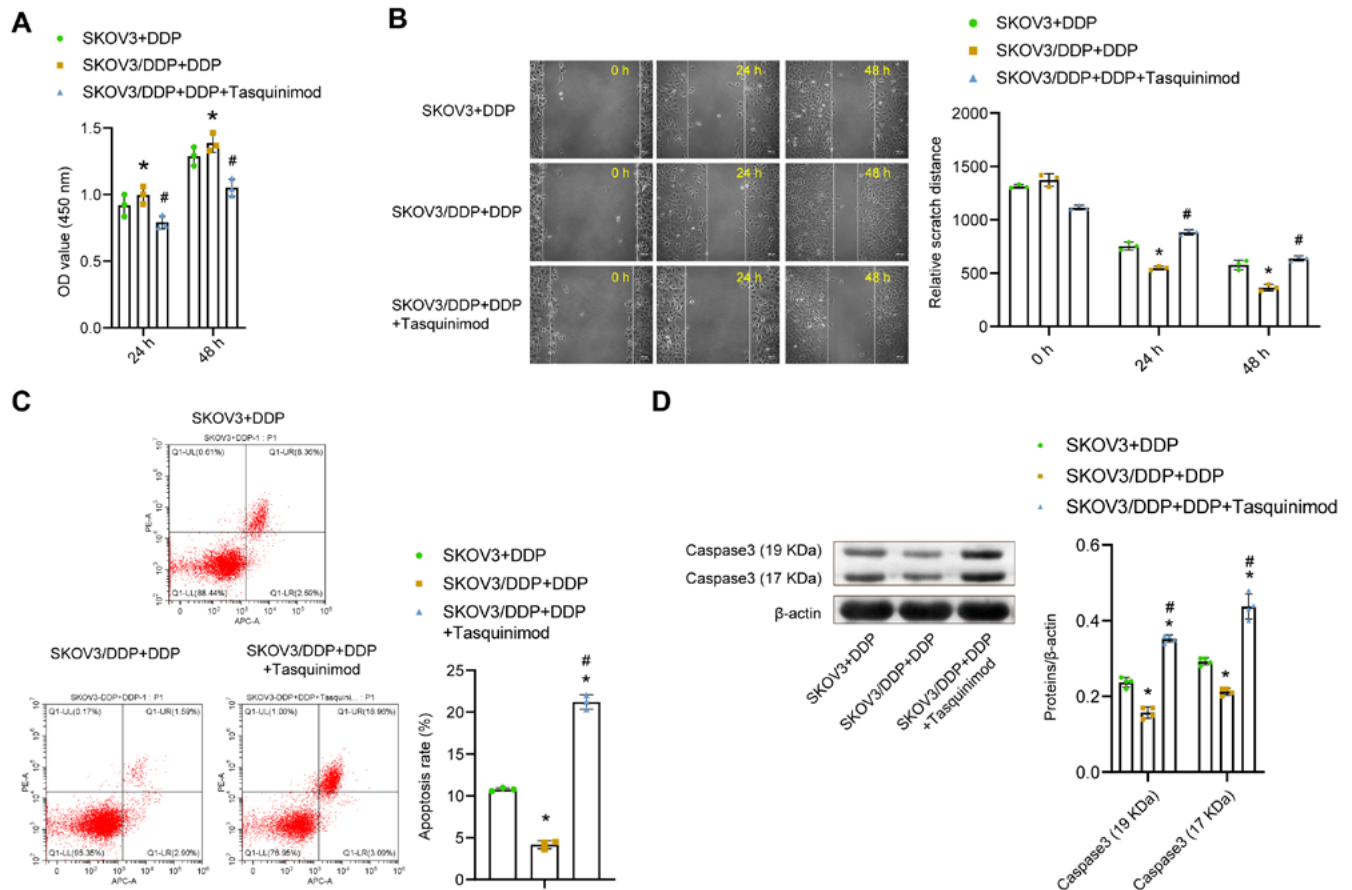


Fig. 4. Tasquinimod increased the sensitivity of SKOV3/DDP cells to cisplatin (DDP). SKOV3 and SKOV3/DDP cell viability was assessed using Cell Counting Kit-8 (CCK-8) (A). The scratch-wound assay was applied to measure the scratch width within 24 h and 48 h (B). In SKOV3 and SKOV3/DDP cells, apoptosis was analyzed with flow cytometry (C). The caspase-3 content was measured with western blot (D) (n = 3 for CCK-8, scratch-wound assay and flow cytometry; n = 4 for western blot (both biological replicates)). Comparisons were made using the one-way analysis of variance (ANOVA) test. In the one-way ANOVA test, $p < 0.05$ illustrated significant differences between the data (* $p < 0.05$ compared to SKOV3+DDP; # $p < 0.05$ compared to SKOV3/DDP+DDP). Data were presented as mean \pm standard deviation (M \pm SD). The scatter point represented the value of a single sample. The details of statistical methods, results and sample size are listed in Supplementary Table 4

OD – optical density.

Tasquinimod induced apoptosis of DDP-resistant ovarian cancer strains by upregulating the Nur77 apoptosis pathway

Next, we determined the relationship between tasquinimod, Nur77 and apoptosis. After the transfection of si-Nur77 into SKOV3/DDP cells, Nur77 expression was significantly decreased, indicating that the transfection with si-Nur77 was successful. Furthermore, compared with the SKOV3/DDP+DDP+tasquinimod+si-NC group, caspase-3 and Nur77 expression in the SKOV3/DDP+DDP+tasquinimod+si-Nur77 group was significantly lower (Fig. 6A,B). Flow cytometry results also showed that apoptosis in the SKOV3/DDP+DDP+si-Nur77 group decreased compared to the SKOV3/DDP+DDP+tasquinimod+si-NC group (Fig. 6C). The effect of tasquinimod was reversed by the si-Nur77 transfection. This indicates that tasquinimod upregulates the Nur77 apoptosis pathway to induce apoptosis in drug-resistant ovarian cancer strains.

Tasquinimod enhanced the anti-tumor effect of DDP in xenografts

To determine the influence of tasquinimod in vivo, we subcutaneously injected SKOV3/DDP cells into nude mice and performed DDP and tasquinimod treatment once the tumor diameter reached 5 mm. The results showed that both tumor volume and diameter gradually increased after subcutaneous injection of SKOV3/DDP cells. The tumor diameter and weight of the SKOV3/DDP+DDP+DDP+tasquinimod group significantly decreased when compared to the SKOV3/DDP+DDP group (Fig. 7A–C). Moreover, western blot results demonstrated that the expression of HDAC4 in the SKOV3/DDP+DDP+DDP+tasquinimod group decreased significantly when compared to the SKOV3/DDP+DDP group, while the levels of Nur77 and Bcl-2 (BH3 domain-specific) demonstrated the opposite (Fig. 7D). These data indicate that tasquinimod enhanced the anti-tumor effect of DDP in xenografts.

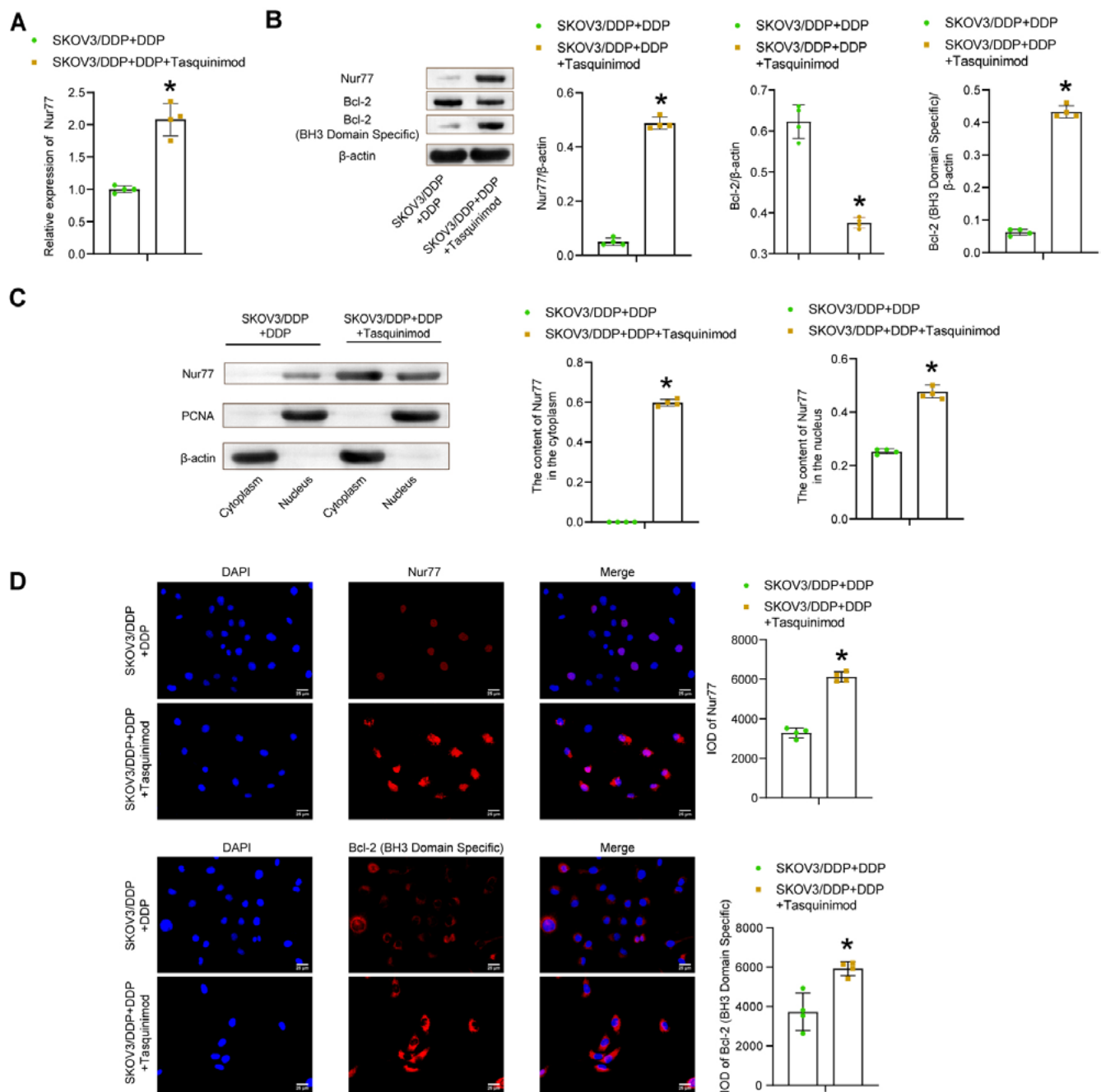


Fig. 5. Tasquinimod affected the Nur77 apoptosis pathway of cisplatin (DDP)-treated ovarian cancer cells. Nur77 expression was detected using quantitative real-time polymerase chain reaction (qPCR) (A) and western blot (B). Nur77, B-cell lymphoma-2 (Bcl-2) and Bcl-2 (BH3 domain-specific) content was detected with western blot (B). Nur77 distribution in cytoplasm or nucleus was detected with western blot (C). Nur77 and Bcl-2 (BH3 domain-specific) distribution were probed with immunofluorescence (IF) (D) ($n = 3$ for IF; $n = 4$ for western blot (both biological replicates)). Comparisons were made using the Mann–Whitney U test or Student's t-test. In the unpaired t-test of Student's t-test or Mann–Whitney U test, $p < 0.05$ illustrated significant differences between the data (* $p < 0.05$ compared to SKOV3/DDP+DDP). Data were presented as mean \pm standard deviation ($M \pm SD$). The scatter point represented the value of a single sample. The details of statistical methods, results and sample size are listed in Supplementary Table 5

Discussion

Cisplatin resistance is an important factor in the high mortality of ovarian cancer.⁴⁸ It is currently a first-line chemotherapy agent for platinum-sensitive ovarian cancer that damages DNA or activates endoplasmic reticulum (ER) stress pathways.⁴⁹ The upregulation of anti-apoptotic pathways is thought to play a crucial role in ovarian cancer drug

resistance.⁷ Therefore, we attempted to influence the apoptosis pathway by regulating HDAC4 expression in order to overcome ovarian cancer drug resistance. In this study, we investigated the effect of tasquinimod on the DDP resistance of SKOV3 and SKOV3/DDP cells, and the association of tasquinimod with the Nur77-Bcl-2 apoptotic pathway. Subsequently, we studied the anti-tumor effect of tasquinimod on DDP in xenografts. We found that HDAC4

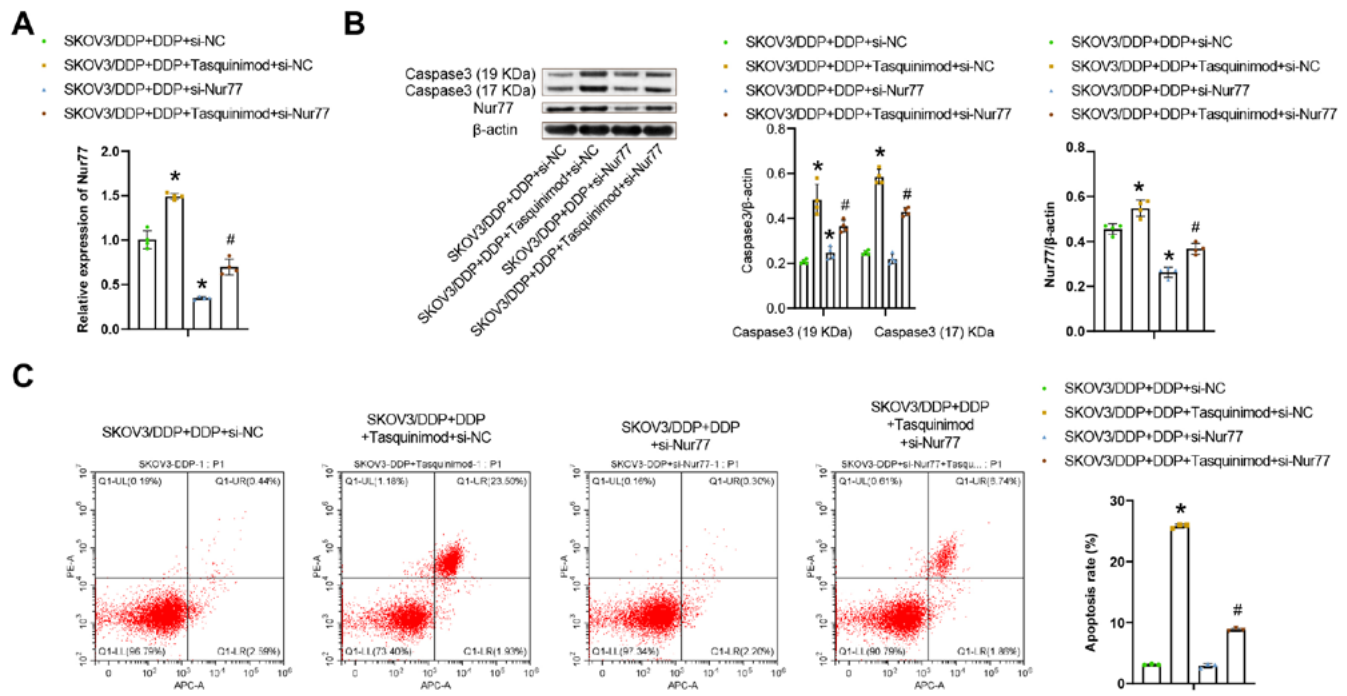


Fig. 6. Tasquinimod induced apoptosis of ovarian cancer drug-resistant strains by upregulating the Nur77 apoptosis pathway. Quantitative real-time polymerase chain reaction (qPCR) was used to measure the Nur77 content (A). Nur77 and caspase-3 content were detected using western blot (B). SKOV3/DDP cell apoptosis was analyzed with flow cytometry (C) ($n = 3$ for flow cytometry; $n = 4$ for qPCR and western blot (both biological replicates)). Comparisons were made using the one-way analysis of variance (ANOVA) test, with $p < 0.05$ illustrating significant differences between the data (* $p < 0.05$ compared to SKOV3/DDP+DDP+si-NC; # $p < 0.05$ compared to SKOV3/DDP+DDP+Tasquinimod+si-NC). Data are presented as mean \pm standard deviation (M \pm SD). The scatter point represented the value of a single sample. The details of statistical methods, results and sample size are listed in Supplementary Table 6

may play a role in regulating ovarian cancer resistance to DDP. After tasquinimod (HDAC4 inhibitor) treatment, ovarian cancer cells showed increased sensitivity to DDP, inhibited growth and increased apoptosis. Tasquinimod upregulated the Nur77-Bcl-2 pathway to induce apoptosis in drug-resistant ovarian cancer cell strains and enhanced the anti-tumor effect of DDP in SKOV3/DDP xenografts.

The HDAC4 is upregulated in a subset of recurrent tumors, including epithelial ovarian cancer (EOC),^{50,51} demonstrating the clinical relevance of the current study.⁵² In particular, HDAC4 was overexpressed in EOC and was connected with poor overall survival of all examined ovarian cancer patients.^{53,54} The HDAC4 also formed protein complexes with HIF1 α that could modulate chemoresistance through protein phosphorylation, translocation and degradation in SKOV3 cells.⁵⁴ We found that HDAC4 level was higher in SKOV3 cells than in IOSE80, and the HDAC4 level was higher in SKOV3/DDP cells than in SKOV3 cells. These results demonstrated that HDAC4 may regulate ovarian cancer resistance to DDP.

Therefore, we treated SKOV3 and SKOV3/DDP cells with tasquinimod. Tasquinimod targets the tumor microenvironment to overcome tumor-associated immunosuppression while inhibiting angiogenesis, metastasis and tumor growth.^{55,56} The inhibitory effects of tasquinimod on tumor-infiltrating immunosuppressive myeloid cells, particularly M2-polarized tumor-associated macrophages (TAMs), have also been observed.^{57,58} Consistently, we found that

tasquinimod, an analog of the HDAC inhibitor, increased cell sensitivity to cisplatin, inhibited growth and promoted apoptosis. Based on this, we hypothesized that the apoptotic pathway regulated by HDAC was related to DDP sensitivity. Previous studies have shown that tasquinimod upregulated the Nur77-Bcl-2 pathway^{59,60} to induce apoptosis in drug-resistant ovarian cancer strains and enhance the anti-tumor effect of DDP in SKOV3/DDP cell xenografts.^{61,62}

A key step in the mitochondrial apoptosis pathway of Nur77 is the interaction of Nur77 with Bcl-2, which induces a conformational change of Bcl-2 and switched Bcl-2 from pro-survival to pro-apoptosis.⁶³ While the growth-promoting role of Nur77 appears to depend on its nuclear role, the death role of Nur77 involved its translocation from the nucleus to the cytoplasm.^{64,65} For example, the death effect of BI1071 was also dependent on the expression of Bcl-2, and BI1071 induced the interaction of Nur77 and Bcl-2.^{11,66} We found increased expression of Nur77 and Bcl-2 (BH3 domain-specific), which were mainly localized in the cytoplasm after tasquinimod induction. Moreover, tasquinimod enhanced the anti-tumor effect of DDP in xenografts.

As a widely used chemotherapy drug in the treatment of breast cancer, DDP has shown good results. However, the development of drug resistance during treatment often leads to treatment failure. Finding new drugs that could be used in clinical resistance is an urgent need, as it could improve the clinical benefits to patients. We found that tasquinimod enhanced the sensitivity of ovarian cancer

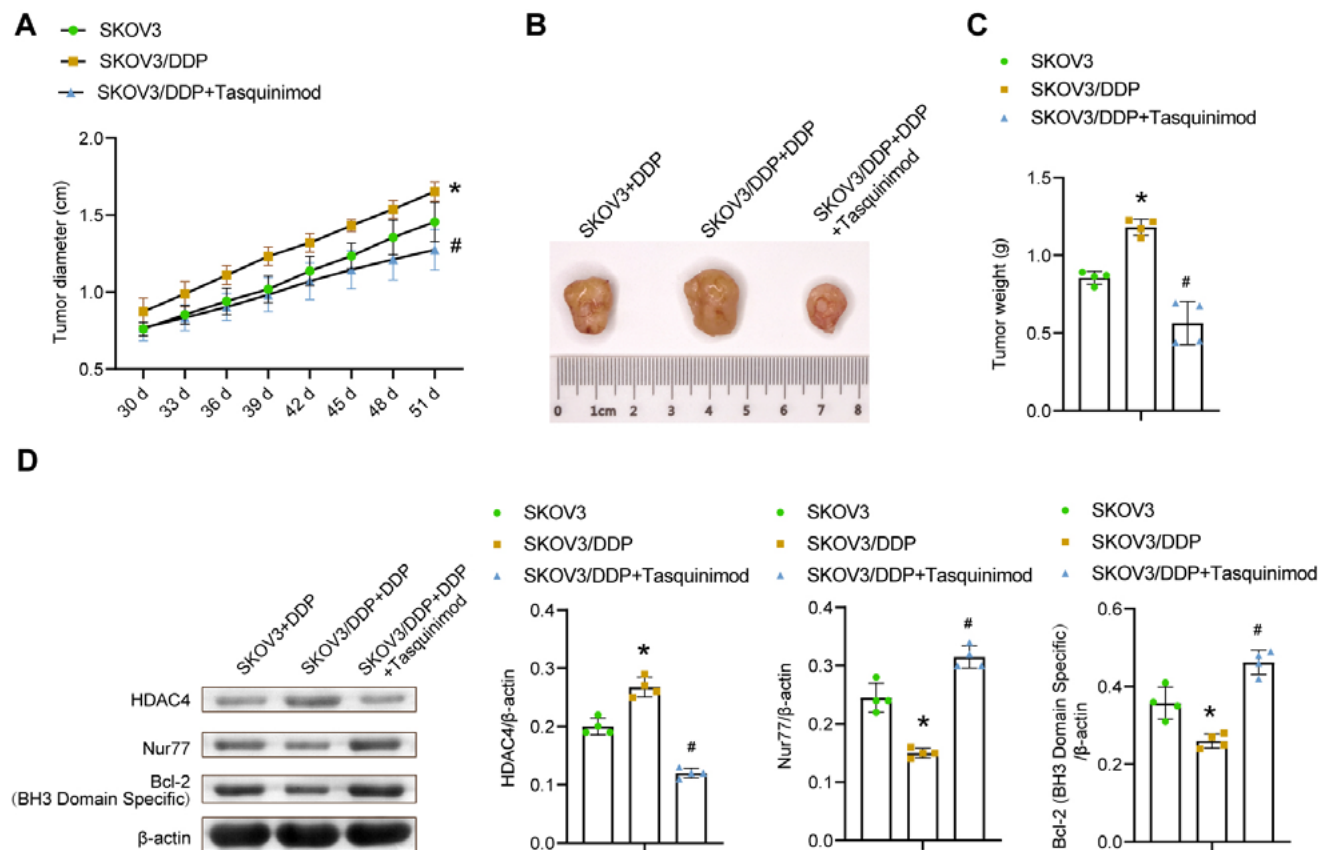


Fig. 7. Tasquinimod enhanced the anti-tumor effect of cisplatin (DDP) in xenografts. Changes in tumor volume of mice (A), typical images of tumors (B) and changes in tumor weight (C) were all measured. The expression changes of histone deacetylase 4 (HDAC4), Nur77 and B-cell lymphoma-2 (Bcl-2) (BH3 domain-specific) were measured using western blot ($n = 4$ for western blot, statistics of tumor volume/weight (both biological replicates)). Comparisons were made using the one-way analysis of variance (ANOVA) test, with $p < 0.05$ illustrating significant differences between the data (* $p < 0.05$ compared to SKOV3+DDP; # $p < 0.05$ compared to SKOV3/DDP+DDP). Data are presented as mean \pm standard deviation ($M \pm SD$). The bar chart showed the M for each group of samples. The error bar represented SD. The scatter point represented the value of a single sample. The details of statistical methods, results and sample size are listed in Supplementary Table 7

cells to DDP by regulating the Nur77-Bcl-2 apoptotic pathway. In future research, it may be necessary to further expand the study sample in order to investigate the effect of tasquinimod (in terms of dose and time) to achieve relief of clinical drug resistance.

Limitations

First, there was a lack of in vivo ovarian cancer staging studies, which is important as the expression of HDAC4/Nur77/Bcl-2 may vary at different tumor stages. Second, we did not explore the relationship between the therapeutic effect of tasquinimod on disease and its dose. We used only a single concentration for exploration in the experiments herein. Third, we did not investigate the relationship between polymorphisms and tasquinimod due to limitations of time and funds.

Conclusions

We found that HDAC4 plays a role in regulating ovarian cancer resistance to DDP. After treatment with

tasquinimod, the sensitivity of ovarian cancer cells to DDP was increased, and the apoptosis rate was decreased. At the molecular level, tasquinimod upregulated the Nur77-Bcl-2 pathway to induce apoptosis in drug-resistant ovarian cancer strains. In vivo mouse studies showed that tasquinimod enhanced the anti-tumor effect of DDP in SKOV3/DDP xenografts. In conclusion, tasquinimod increased the sensitivity of ovarian cancer cells to DDP by regulating the Nur77-Bcl-2 apoptotic pathway.

Supplementary data

The supplementary materials are available at <https://doi.org/10.5281/zenodo.8134377>. The package contains the following files:

Supplementary Table 1. The details of statistical methods, results and sample size for Fig. 1.

Supplementary Table 2. The details of statistical methods, results and sample size for Fig. 2.

Supplementary Table 3. The details of statistical methods, results and sample size for Fig. 3.

Supplementary Table 4. The details of statistical methods, results and sample size for Fig. 4.


Supplementary Table 5. The details of statistical methods, results and sample size for Fig. 5.

Supplementary Table 6. The details of statistical methods, results and sample size for Fig. 6.


Supplementary Table 7. The details of statistical methods, results and sample size for Fig. 7.


ORCID iDs


Ying Lin  <https://orcid.org/0000-0002-0599-1734>

Ya-Qiong Liu  <https://orcid.org/0009-0009-7124-3556>

Ke-An Zhu  <https://orcid.org/0009-0009-6656-6385>

Meng-Qi Hu  <https://orcid.org/0009-0005-4139-5832>

Zhao Li  <https://orcid.org/0009-0007-9448-6484>

Xiao-Jia Min  <https://orcid.org/0000-0001-8093-0969>

References

- Gralewska P, Gajek A, Marczak A, Rogalska A. Participation of the ATR/CHK1 pathway in replicative stress targeted therapy of high-grade ovarian cancer. *J Hematol Oncol*. 2020;13(1):39. doi:10.1186/s13045-020-00874-6
- Budiana ING, Angelina M, Pemayun TGA. Ovarian cancer: Pathogenesis and current recommendations for prophylactic surgery. *J Turkish German Gynecol Assoc*. 2019;20(1):47–54. doi:10.4274/jtgga.galenos.2018.2018.0119
- Liu HD, Xia BR, Jin MZ, Lou G. Organoid of ovarian cancer: Genomic analysis and drug screening. *Clin Transl Oncol*. 2020;22(8):1240–1251. doi:10.1007/s12094-019-02276-8
- Wang JY, Lu AQ, Chen LJ. LncRNAs in ovarian cancer. *Clin Chim Acta*. 2019;490:17–27. doi:10.1016/j.cca.2018.12.013
- Dasari S, Tchounwou PB. Cisplatin in cancer therapy: Molecular mechanisms of action. *Eur J Pharmacol*. 2014;740:364–378. doi:10.1016/j.ejphar.2014.07.025
- Chen SH, Chang JY. New insights into mechanisms of cisplatin resistance: From tumor cell to microenvironment. *Int J Mol Sci*. 2019;20(17):4136. doi:10.3390/ijms20174136
- Lopez A, Reyna DE, Gitego N, et al. Co-targeting of BAX and BCL-XL proteins broadly overcomes resistance to apoptosis in cancer. *Nat Commun*. 2022;13(1):1199. doi:10.1038/s41467-022-28741-7
- Wang J, Zhou JY, Zhang L, Wu GS. Involvement of MKP-1 and Bcl-2 in acquired cisplatin resistance in ovarian cancer cells. *Cell Cycle*. 2009;8(19):3191–3198. doi:10.4161/cc.8.19.9751
- Xu L, Xie Q, Qi L, et al. Bcl-2 overexpression reduces cisplatin cytotoxicity by decreasing ER-mitochondrial Ca^{2+} signaling in SKOV3 cells. *Oncol Rep*. 2017;39(3):985–992. doi:10.3892/or.2017.6164
- Lin B, Kolluri SK, Lin F, et al. Conversion of Bcl-2 from protector to killer by interaction with nuclear orphan receptor Nur77/TR3. *Cell*. 2004;116(4):527–540. doi:10.1016/S0092-8674(04)00162-X
- Banta KL, Wang X, Das P, Winoto A. B cell lymphoma 2 (Bcl-2) residues essential for Bcl-2's apoptosis-inducing interaction with Nur77/Nor-1 orphan steroid receptors. *J Biol Chem*. 2018;293(13):4724–4734. doi:10.1074/jbc.RA117.001101
- Wilson AJ, Liu AY, Roland J, et al. TR3 modulates platinum resistance in ovarian cancer. *Cancer Res*. 2013;73(15):4758–4769. doi:10.1158/0008-5472.CAN-12-4560
- Hu Y, French SW, Chau T, et al. RAR β acts as both an upstream regulator and downstream effector of miR-22, which epigenetically regulates NUR77 to induce apoptosis of colon cancer cells. *FASEB J*. 2019;33(2):2314–2326. doi:10.1096/fj.201801390R
- Tsai C, Liu W, Hsu F, et al. Targeting histone deacetylase 4/ubiquitin-conjugating enzyme 9 impairs DNA repair for radiosensitization of hepatocellular carcinoma cells in mice. *Hepatology*. 2018;67(2):586–599. doi:10.1002/hep.29328
- Tanaka M, Spekter E, Szabó Á, Polyák H, Vécsei L. Modelling the neurodevelopmental pathogenesis in neuropsychiatric disorders: Bioactive kynurenes and their analogues as neuroprotective agents. In celebration of 80th birthday of Professor Peter Riederer. *J Neural Transm*. 2022;129(5–6):627–642. doi:10.1007/s00702-022-02513-5
- Irwin JJ, Shoichet BK. ZINC: A free database of commercially available compounds for virtual screening. *J Chem Inf Model*. 2005;45(1):177–182. doi:10.1021/ci049714+
- Jayathilaka N, Han A, Gaffney KJ, et al. Inhibition of the function of class IIa HDACs by blocking their interaction with MEF2. *Nucl Acids Res*. 2012;40(12):5378–5388. doi:10.1093/nar/gks189
- Wang C, Liu G, Dou G, et al. Z-ligustilide selectively targets AML by restoring nuclear receptors Nur77 and NOR-1-mediated apoptosis and differentiation. *Phytomedicine*. 2021;82:153448. doi:10.1016/j.phymed.2020.153448
- Boros F, Vécsei L. Progress in the development of kynurenine and quinoline-3-carboxamide-derived drugs. *Exp Opin Investig Dugs*. 2020;29(11):1223–1247. doi:10.1080/13543784.2020.1813716
- Martos D, Tuka B, Tanaka M, Vécsei L, Telegdy G. Memory enhancement with kynurenic acid and its mechanisms in neurotransmission. *Biomedicines*. 2022;10(4):849. doi:10.3390/biomedicines10040849
- Li Y, Zhou J, Wang J, Chen X, Zhu Y, Chen Y. Mir-30b-3p affects the migration and invasion function of ovarian cancer cells by targeting the CTHRC1 gene. *Biol Res*. 2020;53(1):10. doi:10.1186/s40659-020-00277-4
- Zhang X, Liu G, Qiu J, Zhang N, Ding J, Hua K. E2F1-regulated long non-coding RNA RAD51-AS1 promotes cell cycle progression, inhibits apoptosis and predicts poor prognosis in epithelial ovarian cancer. *Sci Rep*. 2017;7(1):4469. doi:10.1038/s41598-017-04736-z
- Cao Y, Xie X, Li M, Gao Y. CircHIPK2 contributes to DDP resistance and malignant behaviors of DDP-resistant ovarian cancer cells both in vitro and in vivo through circHIPK2/miR-338-3p/CHTOP ceRNA pathway. *Onco Targets Ther*. 2021;14:3151–3165. doi:10.2147/OTT.S291823
- Olsson A, Björk A, Vallon-Christersson J, Isaacs JT, Leanderson T. Tasquinimod (ABR-215050), a quinoline-3-carboxamide anti-angiogenic agent, modulates the expression of thrombospondin-1 in human prostate tumors. *Mol Cancer*. 2010;9(1):107. doi:10.1186/1476-4598-9-107
- Dalby B, Cates S, Harris A, et al. Advanced transfection with Lipofectamine 2000 reagent: Primary neurons, siRNA, and high-throughput applications. *Methods*. 2004;33(2):95–103. doi:10.1016/j.jymeth.2003.11.023
- Zhang Z, Zhu H, Hu J. CircRAB11FIP1 promoted autophagy flux of ovarian cancer through DSC1 and miR-129. *Cell Death Dis*. 2021;12(2):219. doi:10.1038/s41419-021-03486-1
- Miao JT, Gao JH, Chen YQ, Chen H, Meng HY, Lou G. LncRNA ANRIL affects the sensitivity of ovarian cancer to cisplatin via regulation of let-7a/HMGA2 axis. *Biosci Rep*. 2019;39(7):BSR20182101. doi:10.1042/BSR20182101
- Ding K, Li D, Zhang R, Zuo M. Circ_0047339 promotes the activation of fibroblasts and affects the development of urethral stricture by targeting the miR-4691-5p/TSP-1 axis. *Sci Rep*. 2022;12(1):14746. doi:10.1038/s41598-022-19141-4
- Meng X, Gao X, Chen X, Yu J. Umbilical cord-derived mesenchymal stem cells exert anti-fibrotic action on hypertrophic scar-derived fibroblasts in co-culture by inhibiting the activation of the TGF β 1/Smad3 pathway. *Exp Ther Med*. 2021;21(3):210. doi:10.3892/etm.2021.9642
- Wang X, Zhang Y, Wuyun K, Gong H. Therapeutic effect and mechanism of 4-phenyl butyric acid on renal ischemia-reperfusion injury in mice. *Exp Ther Med*. 2021;23(2):144. doi:10.3892/etm.2021.11067
- Buyandelger B, Bar EE, Hung KS, et al. Histone deacetylase inhibitor MPT0B291 suppresses glioma growth in vitro and in vivo partially through acetylation of p53. *Int J Biol Sci*. 2020;16(16):3184–3199. doi:10.7150/ijbs.45505
- Luchtel RA, Bhagat T, Pradhan K, et al. High-dose ascorbic acid synergizes with anti-PD1 in a lymphoma mouse model. *Proc Natl Acad Sci U S A*. 2020;117(3):1666–1677. doi:10.1073/pnas.1908158117
- Payapilly A, Guilbert R, Descamps T, et al. TIAM1-RAC1 promote small-cell lung cancer cell survival through antagonizing Nur77-induced BCL2 conformational change. *Cell Rep*. 2021;37(6):109979. doi:10.1016/j.celrep.2021.109979
- Zhang J, Liu Z, Dong Y. miR-127-5p targets JAM3 to regulate ferroptosis, proliferation, and metastasis in malignant meningioma cells. *Dis Markers*. 2022;2022:6423237. doi:10.1155/2022/6423237
- Fan QL, Wang JW, Zhang SL, Liu T, Zhao J, You SP. Phenylethanol glycosides protect myocardial hypertrophy induced by abdominal aortic constriction via ECE-1 demethylation inhibition and PI3K/PKB/eNOS pathway enhancement. *Evid Based Complement Alternat Med*. 2020;2020:2957094. doi:10.1155/2020/2957094

36. Scheffler JM, Sparber F, Tripp CH, et al. LAMTOR2 regulates dendritic cell homeostasis through FLT3-dependent mTOR signalling. *Nat Commun*. 2014;5(1):5138. doi:10.1038/ncomms6138
37. Al Haq AT, Tseng HY, Chen LM, Wang CC, Hsu HL. Targeting prooxidant MnSOD effect inhibits triple-negative breast cancer (TNBC) progression and M2 macrophage functions under the oncogenic stress. *Cell Death Dis*. 2022;13(1):49. doi:10.1038/s41419-021-04486-x
38. Msaouel P, Malouf GG, Su X, et al. Comprehensive molecular characterization identifies distinct genomic and immune hallmarks of renal medullary carcinoma. *Cancer Cell*. 2020;37(5):720–734.e13. doi:10.1016/j.ccell.2020.04.002
39. Park Y, Park J, Hwang HJ, et al. Nonsense-mediated mRNA decay factor UPF1 promotes aggresome formation. *Nat Commun*. 2020;11(1):3106. doi:10.1038/s41467-020-16939-6
40. Li P, Xu J, Rao HM, et al. Mechanism of apoptosis induction by mycoplasma nucleolase MGA_0676 in chicken embryo fibroblasts. *Front Cell Infect Microbiol*. 2018;8:105. doi:10.3389/fcimb.2018.00105
41. Brynjolfsson SF, Sigurgrimsdottir H, Einarsdottir ED, et al. Detailed multiplex analysis of SARS-CoV-2 specific antibodies in COVID-19 disease. *Front Immunol*. 2021;12:695230. doi:10.3389/fimmu.2021.695230
42. Yudovich D, Bäckström A, Schmiderer L, Žemaitis K, Subramaniam A, Larsson J. Combined lentiviral- and RNA-mediated CRISPR/Cas9 delivery for efficient and traceable gene editing in human hematopoietic stem and progenitor cells. *Sci Rep*. 2020;10(1):22393. doi:10.1038/s41598-020-79724-x
43. Venâncio C, Félix L, Almeida V, et al. Acute ketamine impairs mitochondrial function and promotes superoxide dismutase activity in the rat brain. *Anesth Analg*. 2015;120(2):320–328. doi:10.1213/ANE.0000000000000539
44. Fay MP, Proschan MA. Wilcoxon–Mann–Whitney or t-test? On assumptions for hypothesis tests and multiple interpretations of decision rules. *Statist Surv*. 2010;4:1–39. doi:10.1214/09-SS051
45. Zimmerman DW, Zumbo BD. Parametric alternatives to the Student t-test under violation of normality and homogeneity of variance. *Percept Mot Skills*. 1992;74(3):835–844. doi:10.2466/pms.1992.74.3.835
46. Wang X, Wang Z, Tang D. Aerobic exercise improves LPS-induced sepsis via regulating the Warburg effect in mice. *Sci Rep*. 2021;11(1):17772. doi:10.1038/s41598-021-97101-0
47. Meah VL, Backx K, Cockcroft JR, Shave RE, Stöhr EJ. Left ventricular mechanics in late second trimester of healthy pregnancy. *Ultrasound Obstet Gynecol*. 2019;54(3):350–358. doi:10.1002/uog.20177
48. Zhang Y, Dong Y, Fu H, et al. Multifunctional tumor-targeted PLGA nanoparticles delivering Pt(IV)/siBIRC5 for US/MRI imaging and overcoming ovarian cancer resistance. *Biomaterials*. 2021;269:120478. doi:10.1016/j.biomaterials.2020.120478
49. Rabik CA, Dolan ME. Molecular mechanisms of resistance and toxicity associated with platinating agents. *Cancer Treat Rev*. 2007;33(1):9–23. doi:10.1016/j.ctrv.2006.09.006
50. Mrkvicova A, Chmellarova M, Peterova E, et al. The effect of sodium butyrate and cisplatin on expression of EMT markers. *PLoS One*. 2019;14(1):e0210889. doi:10.1371/journal.pone.0210889
51. Smith HJ, Straughn JM, Buchsbaum DJ, Arend RC. Epigenetic therapy for the treatment of epithelial ovarian cancer: A clinical review. *Gynecol Oncol Rep*. 2017;20:81–86. doi:10.1016/j.gore.2017.03.007
52. Fan Q, Li L, Wang TL, Emerson RE, Xu Y. A novel ZIP4-HDAC4-VEGFA axis in high-grade serous ovarian cancer. *Cancers*. 2021;13(15):3821. doi:10.3390/cancers13153821
53. Zhou L, Xu X, Liu H, et al. Prognosis analysis of histone deacetylases mRNA expression in ovarian cancer patients. *J Cancer*. 2018;9(23):4547–4555. doi:10.7150/jca.26780
54. Zhang X, Qi Z, Yin H, Yang G. Interaction between p53 and Ras signaling controls cisplatin resistance via HDAC4- and HIF-1 α -mediated regulation of apoptosis and autophagy. *Theranostics*. 2019;9(4):1096–1114. doi:10.7150/thno.29673
55. Raymond E, Dalglish A, Damber JE, Smith M, Pili R. Mechanisms of action of tasquinimod on the tumour microenvironment. *Cancer Chemother Pharmacol*. 2014;73(1):1–8. doi:10.1007/s00280-013-2321-8
56. Leimkühler NB, Gleitz HFE, Ronghui L, et al. Heterogeneous bone-marrow stromal progenitors drive myelofibrosis via a druggable alarmin axis. *Cell Stem Cell*. 2021;28(4):637–652.e8. doi:10.1016/j.stem.2020.11.004
57. Murdoch C, Muthana M, Coffelt SB, Lewis CE. The role of myeloid cells in the promotion of tumour angiogenesis. *Nat Rev Cancer*. 2008;8(8):618–631. doi:10.1038/nrc2444
58. Sawant A, Deshane J, Jules J, et al. Myeloid-derived suppressor cells function as novel osteoclast progenitors enhancing bone loss in breast cancer. *Cancer Res*. 2013;73(2):672–682. doi:10.1158/0008-5472.CAN-12-2202
59. Tu X, Chen X, Zhang D, et al. Optimization of novel oxidative DIMs as Nur77 modulators of the Nur77-Bcl-2 apoptotic pathway. *Eur J Med Chem*. 2021;211:113020. doi:10.1016/j.ejmech.2020.113020
60. Thompson J, Winoto A. During negative selection, Nur77 family proteins translocate to mitochondria where they associate with Bcl-2 and expose its proapoptotic BH3 domain. *J Exp Med*. 2008;205(5):1029–1036. doi:10.1084/jem.20080101
61. Zhong Y, Le F, Cheng J, et al. Triptolide inhibits JAK2/STAT3 signaling and induces lethal autophagy through ROS generation in cisplatin-resistant SKOV3/DDP ovarian cancer cells. *Oncol Rep*. 2021;45(5):69. doi:10.3892/or.2021.8020
62. Hu H, Zhu S, Tong Y, Huang G, Tan B, Yang L. Antitumor activity of triptolide in SKOV3 cells and SKOV3/DDP in vivo and in vitro. *Anticancer Drugs*. 2020;31(5):483–491. doi:10.1097/CAD.0000000000000894
63. Kolluri SK, Zhu X, Zhou X, et al. A short Nur77-derived peptide converts Bcl-2 from a protector to a killer. *Cancer Cell*. 2008;14(4):285–298. doi:10.1016/j.ccr.2008.09.002
64. Lee SO, Andey T, Jin UH, Kim K, Sachdeva M, Safe S. The nuclear receptor TR3 regulates mTORC1 signaling in lung cancer cells expressing wild-type p53. *Oncogene*. 2012;31(27):3265–3276. doi:10.1038/onc.2011.504
65. Peng SZ, Chen XH, Chen SJ, et al. Phase separation of Nur77 mediates celastrol-induced mitophagy by promoting the liquidity of p62/SQSTM1 condensates. *Nat Commun*. 2021;12(1):5989. doi:10.1038/s41467-021-26295-8
66. Chen X, Cao X, Tu X, et al. BI1071, a novel Nur77 modulator, induces apoptosis of cancer cells by activating the Nur77-Bcl-2 apoptotic pathway. *Mol Cancer Ther*. 2019;18(5):886–899. doi:10.1158/1535-7163.MCT-18-0918